


Dorsal attention network activity during perceptual organization is distinct in schizophrenia and predictive of cognitive disorganization

Brian P. Keane^{1,2}  | Bart Krekelberg³ | Ravi D. Mill³ |
Steven M. Silverstein^{1,2,4} | Judy L. Thompson^{2,5} | Megan R. Serody^{1,2} |
Deanna M. Barch⁶ | Michael W. Cole³

¹University Behavioral Health Care, Department of Psychiatry, and Center for Cognitive Science, Rutgers, The State University of New Jersey, Piscataway, New Jersey, USA

²Departments of Psychiatry and Neuroscience, University of Rochester Medical Center, Rochester, New York, USA

³Center for Molecular and Behavioral Neuroscience, Rutgers, The State University of New Jersey, Newark, New Jersey, USA

⁴Department of Ophthalmology, University of Rochester Medical Center, Rochester, New York, USA

⁵Department of Psychiatric Rehabilitation and Counseling Professions, Rutgers, The State University of New Jersey, Piscataway, New Jersey, USA

⁶Departments of Psychological & Brain Sciences, Psychiatry, and Radiology, Washington University in St. Louis, St. Louis, Missouri, USA

Correspondence

Brian P. Keane, University Behavioral Health Care, Department of Psychiatry, and Center for Cognitive Science, Rutgers, The State University of New Jersey, Piscataway, NJ 08854, USA.
Email: brian_keane@urmc.rochester.edu

Funding information

National Institute of Mental Health, Grant/Award Number: K01MH108783

Abstract

Visual shape completion is a canonical perceptual organization process that integrates spatially distributed edge information into unified representations of objects. People with schizophrenia show difficulty in discriminating completed shapes, but the brain networks and functional connections underlying this perceptual difference remain poorly understood. Also unclear is whether brain network differences in schizophrenia occur in related illnesses or vary with illness features transdiagnostically. To address these topics, we scanned (functional magnetic resonance imaging, fMRI) people with schizophrenia, bipolar disorder, or no psychiatric illness during rest and during a task in which they discriminated configurations that formed or failed to form completed shapes (illusory and fragmented condition, respectively). Multivariate pattern differences were identified on the cortical surface using 360 predefined parcels and 12 functional networks composed of such parcels. Brain activity flow mapping was used to evaluate the likely involvement of resting-state connections for shape completion. Illusory/fragmented task activation differences ('modulations') in the dorsal attention network (DAN) could distinguish

Abbreviations: AUC, area under the curve; BP, bipolar disorder; CDSS, Calgary Depression Scale for Schizophrenia; DAN, dorsal attention network; DCM, dynamic causal modeling; EPI, echo-planar imaging; FDR, false discovery rate; HC, healthy control; MAE, mean absolute error; MVPA, multivariate pattern analysis; PANSS, Positive and Negative Syndrome Scale; PAS, Premorbid Adjustment Scale; PCA, Principal Component Analysis; RSFC, resting-state functional connectivity; SLOF, Specific Level of Functioning Scale; SZ, schizophrenia; YMRS, Young Mania Rating Scale.

Deanna M. Barch and Michael W. Cole are co-senior authors.

people with schizophrenia from the other groups (AUCs > .85) and could transdiagnostically predict cognitive disorganization severity. Activity flow over functional connections from the DAN could predict secondary visual network modulations in each group, except in schizophrenia. The secondary visual network was strongly and similarly modulated in each group. Task modulations were dispersed over more networks in patients compared to controls. In summary, DAN activity during visual perceptual organization is distinct in schizophrenia, symptomatically relevant, and potentially related to improper attention-related feedback into secondary visual areas.

KEYWORDS

bipolar disorder, illusory contours, resting-state functional connectivity, shape completion, top-down

1 | INTRODUCTION

Schizophrenia (SZ) is a debilitating disorder characterized by delusions, hallucinations, disorganized thought and a decline in social/occupational functioning. The disorder also adversely impacts aspects of visual perceptual organization (Silverstein & Keane, 2011) and, in particular, visual shape completion, which builds shape representations from co-aligned step-edge elements (Keane et al., 2019). Why might this be? The question is important because shape completion plays a fundamental role for normal seeing (Keane, 2018), recovering object shape, size and number from camouflaged or cluttered distal environments. Understanding subtle impairments in shape completion and related perceptual organization processes could, for example, help explain why individuals with the disorder have uncomfortable sensations of sensory flooding (Bunney et al., 1999) or poorer overall day-to-day visual functioning (Shoham et al., 2020). Another reason to investigate the brain-basis of shape completion in SZ is that the underlying mechanisms in healthy individuals are already partly understood. Extensive investigations in human and non-human primates using single-unit recording, transcranial magnetic stimulation (TMS), electroencephalography (EEG) and functional magnetic resonance imaging (fMRI), have all shown that shape completion relies upon mid-level visual regions such as lateral occipital cortex and V4, as well as recursive interactions with V1 and V2 (Chen et al., 2020; Cox et al., 2013; Murray et al., 2006). Recent neuroimaging efforts have additionally revealed that shape completion activates a sparse but densely interconnected coalition of regions that is seated in the secondary visual network and that incorporates parts of at least four other networks (Keane, Barch, et al., 2021). Neuroimaging

results in SZ can be understood within this existing literature.

We postulated on the basis of past work that SZ patients can form illusory contours at initial stages of processing but do not properly use such contours at later, conceptual stages. As evidence, in a visual evoked potential study, when participants discriminated configurations that formed or failed to form illusory shapes, there was an intact illusory contour formation waveform over lateral occipital regions at 106–194 ms post-stimulus onset (see also, Wynn et al., 2015) and an increased, possibly compensatory, ‘closure negativity’ waveform across frontal regions at 240–400 ms. In a methodologically similar EEG study, when subjects discriminated illusory square from non-illusory (fragmented) stimuli, SZ patients exhibited a unique response-locked high-gamma oscillation—with a fronto-temporal topography—at a relatively late processing stage (100 ms before button-press) (Spencer & Ghorashi, 2014). In a psychophysical study, SZ patients reacted normally to distractor lines placed near illusory contours, suggesting intact illusory contour formation, but were overall poor at discriminating illusory shapes, suggesting a lessened ability to notice and use illusory contours (Keane et al., 2014; Keane, Erlikhman, et al., 2021). In a non-clinical psychophysical study, when participants were cognitively biased through instructional templates and verbal instructions to see the inducing pac-man edges as disconnected, they performed as if they had SZ; that is, they normally reacted to distractor lines, normally discriminated non-illusory stimuli (which failed to form illusory contours), but poorly discriminated illusory shapes (Keane et al., 2012). The foregoing results, taken together, suggest that patients’ visual networks may operate relatively normally during shape completion but that higher-order cognitive networks may

not. A purpose of the present investigation is to test this assertion with functional MRI.

A second goal was to consider whether the implicated cognitive control networks would be related to cognitive disorganization. Disorganization was of interest because this symptom type, but not others, has been linked to poor shape completion (Keane et al., 2019). Disorganization has also been associated with gamma band oscillation abnormalities during the discrimination of illusory and fragmented shapes (Spencer et al., 2004; Spencer & Ghorashi, 2014).

Finally, as a more exploratory measure, we investigated the extent to which top-down feedback might influence activity in the secondary visual network during shape completion, given the critical role of this network for shape completion (Keane, Barch, et al., 2021). We have provided evidence that—in healthy controls—the dorsal attention network (DAN) plausibly acts as a bridge to the secondary visual network and we have supported this claim with a ‘brain activity flow’ modelling procedure (‘ActFlow’) in which task activations and resting-state functional connections from the DAN could be used to model task activations in the secondary visual network (Cole et al., 2016; Keane, Barch, et al., 2021). There are reasons to think that such feedback should be weak in SZ. Dynamic causal modelling has shown that—during a depth inversion illusion task—SZ patients exhibited poor top-down feedback from the intraparietal sulcus (overlapping with the DAN) to the lateral occipital cortex (in the secondary visual network) but normal feedforward activity between the same regions (Dima et al., 2010). Other studies have shown intact subliminal processing of masked words or digits, indicating potentially preserved bottom-up processing (Berkovitch et al., 2017). If top-down feedback is indeed impaired in SZ, then the above-described modelling effort should not be successful for the secondary visual network in SZ.

To address the above three questions, we scanned 16 SZ participants and 15 people with bipolar disorder (BP). These results were compared to healthy control data ($n = 20$) that were already reported in an earlier study (Keane, Barch, et al., 2021). Bipolar disorder was considered because it offers an important foil for SZ. Over 40% of bipolar disorder patients take antipsychotic medications (Rhee et al., 2020), over half report at least one lifetime psychotic symptom (Dunayevich & Keck, 2000), both are associated with chronic medical problems and past substance abuse history (Cassidy et al., 2001; Dixon, 1999), and there is genetic overlap between the two (Lichtenstein et al., 2009). Therefore, establishing group differences between SZ and bipolar disorder would rule out potential confounds and more convincingly demonstrate specificity to SZ. Including a

bipolar disorder group also allowed us to determine whether brain network activity could predict cognitive disorganization severity transdiagnostically.

We investigated brain network differences in shape completion with four task scans and one resting-state scan. In the task scans, participants discriminated pacman configurations that formed or failed to form visually completed shapes (illusory and fragmented condition, respectively) (Ringach & Shapley, 1996). Similar to past studies, shape completion was operationalized as the difference in performance or activation between the illusory and fragmented conditions (Keane et al., 2019; Keane, Barch, et al., 2021). The resting-state scan allowed us to compute the resting-state functional connectivity (RSFC) matrix between all pairs of regions, which in turn allowed us to model top-down feedback into the secondary visual network via a brain activity flow mapping procedure (‘ActFlow’; see Section 2) (Cole et al., 2016). The ActFlow approach is justified since task and rest generate highly similar brain-wide functional connectivity (Cole et al., 2014) and since integrating RSFC into ActFlow has yielded accurate inferences of task evoked activations in previous studies (Cole et al., 2016).

Sample size limitations were mitigated in several ways. First, because all analyses were conducted on networks rather than individual regions, we could reduce the number of multiple comparisons, pool over functionally related cortical areas, and thereby dramatically improve power (Cremers et al., 2017; Ji et al., 2019; Noble et al., 2022; Rosenberg et al., 2015). Second, we used cross-validation and permutation testing to avoid overfitting (Scheinost et al., 2019). Third, the major positive results could withstand Bonferroni correction and the major negative results (with the visual networks) held true before statistical correction. The disorganization symptom prediction was evaluated with the full patient sample ($n = 31$). Finally, as already described, key predictions were motivated by—and fit within—past literature.

2 | MATERIALS AND METHODS

2.1 | Participants

The sample consisted of 20 healthy controls (HCs), 15 people with bipolar disorder (BPs; type I, type II, and 1 unspecified), and 16 people with SZ including one with schizoaffective disorder (SZs; see Table 1). The control data were separately published to establish the normal brain network mechanisms of shape completion and to set the stage for patient comparisons (Keane, Barch, et al., 2021). One control and one bipolar participant

TABLE 1 Demographic and clinical characteristics of participants

Variable	HC (<i>n</i> = 20)		BP (<i>n</i> = 15)		SZ (<i>n</i> = 16)		Group comp.	Pairwise comparisons (uncorrected)
	Mean or percent	SD	Mean or percent	SD	Mean or percent	SD	<i>p</i>	
Age (years)	37.6	11.2	39.7	8.6	40.3	7.6	.660	
Education, parental average (years)	12.8	2.7	13.5	2.1	13.0	4.1	.812	
Education, self (years)	14.9	2.6	14.6	1.7	13.0	3.4	.105	
FSIQ (Shipley-2)	100.5	9.9	105.7	5.8	95.6	14.4	.040	SZ < BP*
Gender (% male)	60		33		69		.118	
Handedness (% right)	80		87		88		.515	
Smoking habits (% smokers)	17		43		47		.137	
Nicotine dependence	21.3	5.5	19.7	7.5	20.1	7.8	.95	
Antipsychotic type: Typical/atypical/both (%)			0/100/0		14/79/7		.262	
Olanzapine equiv. (mg/day)			6.4	10.6	14.1	14.5	.103	
Imipramine equiv. (mg/day)			41.7	69.9	31.9	71.8	.703	
Lithium equiv. (mg/day)			803.9	654.8	216.9	412.3	.005	
Functioning, current (SLOF)			4.1	.6	4.1	.5	.736	
Functioning, premorbid (PAS)			.22	.10	.28	.18	.294	
Illness duration (years)			20.0	10.9	15.7	9.3	.249	
Illness onset age (years)			19.6	9.5	22.3	9.2	.458	
CDSS, total			6.9	6.3	4.7	3.6	.250	
Schizo-Bipolar Scale, total			1.7	1.8	7.6	1.5	<.001	
YMRS, total			2.9	2.6	9.1	6.6	.002	
PANSS, positive			1.4	.6	2.8	1.1	<.001	
PANSS, negative			1.6	.7	1.8	.6	.318	
PANSS, disorganized			1.8	.4	2.3	.8	.045	
PANSS, excitement			1.7	.5	1.8	.5	.498	
PANSS, depression			3.5	1.5	3.2	1.1	.586	
PANSS, total			1.7	.4	2.2	.4	.001	

Note: FSIQ = Full-Scale IQ. SLOF = Specific Levels of Functioning Scale mean score per scorable item (1–5, with 5 being highest functioning). The Faergstrom Test of Nicotine Dependence scores were only reported for subjects who smoked. Antipsychotic type pertains only to those who were using antipsychotics. PAS = Premorbid Adjustment Scale, averaged across age period (with higher scores denoting more dysfunction). CDSS = Calgary Depression Scale for Schizophrenia. YMRS = Young Mania Rating Scale. PANSS = Positive and Negative Syndrome Scale mean score per item. Interval/ordinal variables were compared with ANOVAs/*t* tests. Frequency statistics (e.g., handedness and gender) were measured with Chi-square or Fisher's exact test (i.e., on 2 × 2 tables). Note that the bipolar disorder participants scored lower on the YMRS because they were not manic at the time of testing (being in a manic state was an exclusionary criterion) and because some manic symptoms overlap with psychosis, namely, hallucinations, delusions and conceptual disorganization.

**p* < .05.

lacked resting-state data but were still included in the task analyses. Patients were recruited from the Newark and Piscataway outpatient and partial hospital clinics at

Rutgers University Behavioral Health Care (with one exception being a SZ patient from the Nathan Kline Institute in Orangeburg NY). Controls were recruited from

the same metropolitan areas. To prevent exaggerated group differences in IQ and education, controls without four-year college degrees were preferentially recruited. As can be seen from Table 1, groups did not differ on age, education (self/parental), smoking habits, handedness or gender; the patient groups did not differ on illness duration, olanzapine/imipramine equivalents or current/premorbid functioning.

The inclusion/exclusion criteria for all subjects were (1) age 21–55; (2) no electroconvulsive therapy in the past 8 weeks; (3) no neurological or pervasive developmental disorders; (4) no recent substance use disorder (i.e., participants must not have satisfied more than one of the 11 Criterion A symptoms of DSM-5 substance use disorder in the last 3 months); (5) no positive urine toxicology screen or breathalyser test on any day of testing, including THC; (6) no brain injury due to accident or illness (e.g., stroke or brain tumour) and no accompanying loss of consciousness for more than 10 min; (7) no amblyopia (as assessed by informal observation and self-report); (8) visual acuity of 20/32 or better (with corrective lenses if necessary); (9) the ability to understand English and provide written informed consent; (10) no scanner related contraindications (no claustrophobia, an ability to fit within the scanner bed and no non-removable ferromagnetic material on or within the body); (11) no intellectual impairment (IQ < 70) as assessed with a brief vocabulary test (Shipley-2; see below). Additional criteria for controls were: (1) no DSM-5 diagnosis of past or current psychotic or mood disorders (including past mood episode); (2) no current psychotropic- or cognition-enhancing medication; (3) no first-degree relative with SZ, schizoaffective, or bipolar disorder (as indicated by self-report). Additional criteria for patients were (1) a DSM-5 diagnosis of SZ, schizoaffective (depressive subtype) or bipolar disorder. Patients could not be in a manic state at the time of testing.

Written informed consent was obtained from all subjects after explanation of the nature and possible consequences of participation. The study followed the tenets of the Declaration of Helsinki and was approved by the Rutgers University Institutional Review Board. All participants received monetary compensation and were naive to the study's objectives.

2.2 | Assessments

Psychiatric diagnosis was assessed with the Structured Clinical Interview for DSM-5 (SCID; 28) and was assigned only after consulting detailed medical history and the SCID. All diagnoses were further considered during a weekly diagnostic consensus meeting. All clinical

instruments were administered by a rater who had established reliability with raters in other ongoing studies (e.g., ICC > .8).

Intellectual functioning of all subjects was assessed with a brief vocabulary test that correlates highly ($r = .80$) with WAIS-III full-scale IQ scores (Canivez & Watkins, 2010; W. C. Shipley et al., 2009, p. 65). Visual acuity was measured with a logarithmic visual acuity chart under fluorescent overhead lighting (viewing distance = 2 m, lower limit = 20/10), and in-house visual acuity correction was used for individuals without appropriate glasses or contacts. The Alere iCup Dx Drug Screen Cup was utilized to probe for the presence of recreational and illicit substances (i.e., THC, cocaine, methamphetamines, amphetamines and opiates). The AlcoHawk Pro breathalyser was administered to test for recent alcohol consumption. All included subjects tested negative for each test at the time of scanning. Nicotine use was assayed with the Faegerstrom Test for Nicotine Dependence (Heatherston et al., 1991). Standardized medication dose equivalents (olanzapine, lithium and imipramine equivalents) were determined for each patient using published tables (Bollini et al., 1999; Gardner et al., 2010) (Table 1).

The Positive and Negative Syndrome Scale (PANSS; Kay et al., 1987) was administered within 2 weeks of the scan and provided information about symptoms over the last 2 weeks. PANSS symptom scores were reported via a 'consensus' five-factor model, which was designed on the basis of 29 previous five-factor models (Wallwork et al., 2012). The disorganization score was the clinical variable of greatest interest, given its previously documented relation to shape completion (Keane et al., 2019).

To fully characterize the patient samples, we also administered several other symptom/functioning assessments. Depressive and manic symptoms were assessed with the Calgary Depression Scale for Schizophrenia (CDSS; D. Addington et al., 1993) and the Young Mania Rating Scale (YMRS; Young et al., 1978), respectively. The Specific Levels of Functioning Scale (SLOF; Schneider & Struening, 1983) estimated day-to-day functioning in areas such as physical functioning, personal care, interpersonal relationships, social acceptability, activities and work skills. The Premorbid Adjustment Scale (PAS; Cannon-Spoor et al., 1982) measured sociability, peer relationship quality, scholastic performance, school adaptation and (where appropriate) social-sexual functioning up to 1 year before illness onset; this was done for childhood (up through age 11), early adolescence (ages 12–15), late adolescence (ages 16–18) and adulthood (ages 19 and above). In line with what others have done, the PAS General score was not included since it is reflective of functioning before and after illness onset

(van Mastrigt & Addington, 2002). For individuals with SZ, illness onset on the PAS was defined as when one or more positive symptoms first became noticeable or concerning to the patient. For individuals with bipolar disorder, illness onset was defined as the onset of the first mood episode (either manic or major depressive). Each patient's position along the schizo-bipolar spectrum was assessed with the Schizo-Bipolar Scale (Keshavan et al., 2011). Higher scores indicated that a subject was more towards the pure 'schizophrenia' end of the spectrum.

2.3 | Experimental design and statistical analysis

2.3.1 | Stimulus and procedure

Participants performed a 'fat/thin' shape discrimination task in which they indicated whether four pac-men formed a fat or thin shape ('illusory' condition) or whether four downward-facing pac-men were uniformly rotated left or right ('fragmented' condition) (see Figure 1). This so-called 'fat/thin' task was chosen because it has been used extensively to investigate shape completion via psychophysics, fMRI, EEG and TMS (Maertens & Pollmann, 2005; Murray et al., 2006; Pillow & Rubin, 2002; Wokke et al., 2013) and because it has also been used to demonstrate shape completion deficits in past behavioral work in SZ (Keane et al., 2019). The fragmented task is a suitable control in that it involves judging the lateral properties of the stimulus—just like the illusory condition—and in that it uses groupable elements (via common orientation, Beck, 1966). As described elsewhere (Keane, Barch, et al., 2021), the two tasks shared most stimulus and procedural details (stimulus timing, pac-man features, spatial distribution, etc.) and therefore relied on many of the same processes (temporal attention, divided attention, visual working memory, etc.) (Keane et al., 2019). Perhaps because of these similarities, the tasks generate similar performance thresholds, reaction times, and accuracies, and are highly correlated behaviorally (Keane et al., 2019; Keane, Barch, et al., 2021), which is interesting since extremely similar visual tasks are often uncorrelated even within large samples (Grzechowski et al., 2017). In sum, by having employed a closely matched and already tested control condition, we were in a position to judge mechanisms relatively unique to shape completion.

Subjects viewed the stimuli in the scanner from a distance of 99 cm by way of a mirror attached to the head coil. There were four white sector circles (radius = .88°, or 60 pixels) centred at the vertices of an

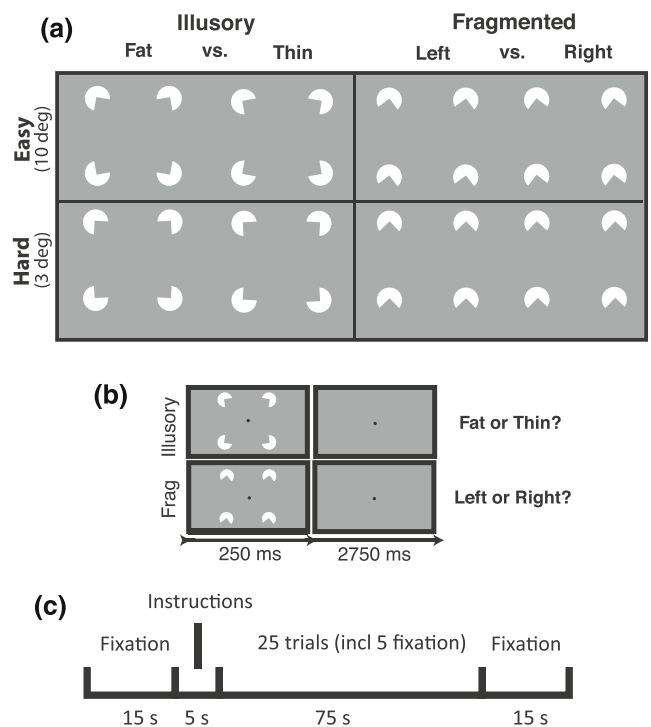


FIGURE 1 Stimuli, trial sequence and block arrangement for the visual shape completion experiment. (a) Sector circles (pac-men) were oriented to generate visually completed shapes (illusory condition) or fragmented configurations that lacked interpolated boundaries (fragmented condition). There were two difficulty conditions corresponding to the amount by which the pac-men were individually rotated to create the response alternatives. (b) After briefly seeing the target, subjects responded with a button press. (c) Each half of a run (out of a total of four runs) consisted of a fixation screen, a 5-s instructional screen, 25 trials of a single task condition (including five fixation trials), and then another fixation screen. Figure re-used from Keane, Barch, et al. (2021).

invisible square (side = 5.3°, or 360 pixels), which itself was centred on a grey screen (see Figure 1). Stimuli were initially generated with MATLAB and Psychtoolbox code (Pelli, 1997) with anti-aliasing applied for edge artifact removal. Images were subsequently presented in the scanner via PsychoPy (version 1.84; Peirce, 2007) on a MacBook Pro. Illusory contour formation depended on the geometric property of 'reliability' (Kellman & Shipley, 1991): when the pac-men were properly aligned (reliable), the illusory contours were present (the 'illusory' condition); when misaligned (unreliable), they were absent ('fragmented' condition).

Within each of the four runs, there was one block of each task condition. Block ordering (illusory/fragmented or vice versa) alternated from one run to the next and the initial block sequence was counterbalanced across observers (illusory first or fragmented first). Each block had two difficulty levels, corresponding to the magnitude

of pac-man rotation ($\pm 10^\circ$ 'easy', or $\pm 3^\circ$ of rotation, 'hard'). Within each block, there were 20 task trials and five fixation trials. Half of the task trials were easy, and half were hard; half of these two trial types were illusory, and half were fragmented. The ordering of these trial types (including fixation) was counterbalanced. Each trial consisted of a 250-ms pac-man stimulus (task trial) or 250-ms fixation dot (fixation trial), followed by a 2750-ms fixation dot. Subjects needed to issue a response before the end of a task trial; otherwise, a randomly selected response was assigned at the end of that trial and the following trial ensued. Feedback was provided at the end of each run in the form of accuracy averaged cumulatively across all test trials.

Subjects received brief practice outside of and within the scanner before the actual experiment. During practice, subjects were reminded orally and in writing to keep focused on a centrally-appearing fixation point for each trial. To ensure that subjects thoroughly understood the task, pictures of the fat/thin stimuli were shown side-by-side and in alternation so that the differences could be clearly envisaged. Subjects issued responses with a two-button response device that was held on their abdomens with their dominant hand. Subjects practiced with this same type of device outside of the scanner. Feedback after each trial was provided during the practice phase only (correct, incorrect and slow response).

2.3.2 | fMRI acquisition

Data were collected at the Rutgers University Brain Imaging Center (RUBIC) on a Siemens Tim Trio scanner. Whole-brain multiband echo-planar imaging (EPI) acquisitions were collected with a 32-channel head coil with TR = 785 ms, TE = 34.8 ms, flip angle = 55° , bandwidth 1894/Hz/Px, in-plane FoV read = 211 mm, 60 slices, 2.4-mm isotropic voxels, with GRAPPA (PAT = 2) and multiband acceleration factor 6. Note that multiband fMRI data boosts signal-to-noise ratio (SNR) due to its higher temporal resolution, and generates less signal dropout near the ventral surface due to its higher spatial resolution (Merboldt et al., 2000; Smith et al., 2013). Whole-brain high-resolution T1-weighted and T2-weighted anatomical scans were also collected with .8-mm isotropic voxels. Spin echo field maps were collected in both the anterior-to-posterior and posterior-to-anterior directions in accordance with the Human Connectome Project preprocessing pipeline (version 3.25.1) (Glasser et al., 2013). After excluding dummy volumes to allow for steady-state magnetization, each experimental functional scan spanned 3 min and 41 s (281 TRs). Scans were collected consecutively with short breaks in

between (subjects did not leave the scanner). An additional 10-min resting-state scan (765 TRs) occurred in a separate session, with the same pulse sequence. Note that due to scanner time constraints one SZ participant finished only 751 of the 765 TRs.

2.3.3 | fMRI preprocessing and functional network partition

Preprocessing steps have been reported previously (Keane, Barch, et al., 2021) but are repeated below. Imaging data were preprocessed using the publicly available Human Connectome Project minimal preprocessing pipeline, which included anatomical reconstruction and segmentation; and EPI reconstruction, segmentation, spatial normalization to standard template (including surface-based smoothing with a 2-mm FWHM filter), intensity normalization, and motion correction (Glasser et al., 2013). All subsequent preprocessing steps and analyses were conducted on CIFTI 64k grayordinate standard space. This was done for the parcellated time series using the Glasser et al. (2016) atlas (i.e., one BOLD time series for each of the 360 cortical parcels, where each parcel averaged over vertices). The Glasser surface-based cortical parcellation combined multiple neuroimaging modalities (i.e., myelin mapping, cortical thickness, task fMRI and RSFC) to improve confidence in cortical area assignment. The parcellation thus provided a principled way to parse the cortex into manageable number of functionally meaningful units and thereby reduce the number of statistical comparisons. These same parcels were also used to construct the brain network partition described further below.

We performed nuisance regression on the minimally preprocessed task data using 24 motion parameters (six motion parameter estimates, their derivatives, and the squares of each) and the four ventricle and four white matter parameters (parameter estimates, the derivatives, and the squares of each) (Ciric et al., 2017). For the task scans, global signal regression, motion scrubbing, spatial smoothing (other than mentioned above), and temporal filtering were not used. Each run was individually demeaned and detrended (two additional regressors per run).

The resting-state scans were preprocessed in the same way as the parcellated task data (including the absence of global signal regression) except that we removed the first five frames and applied motion scrubbing (Power et al., 2012). That is, whenever the framewise displacement for a particular frame exceeded .3 mm, we removed that frame, one prior frame, and two subsequent frames (Schultz et al., 2018). Framewise displacement was

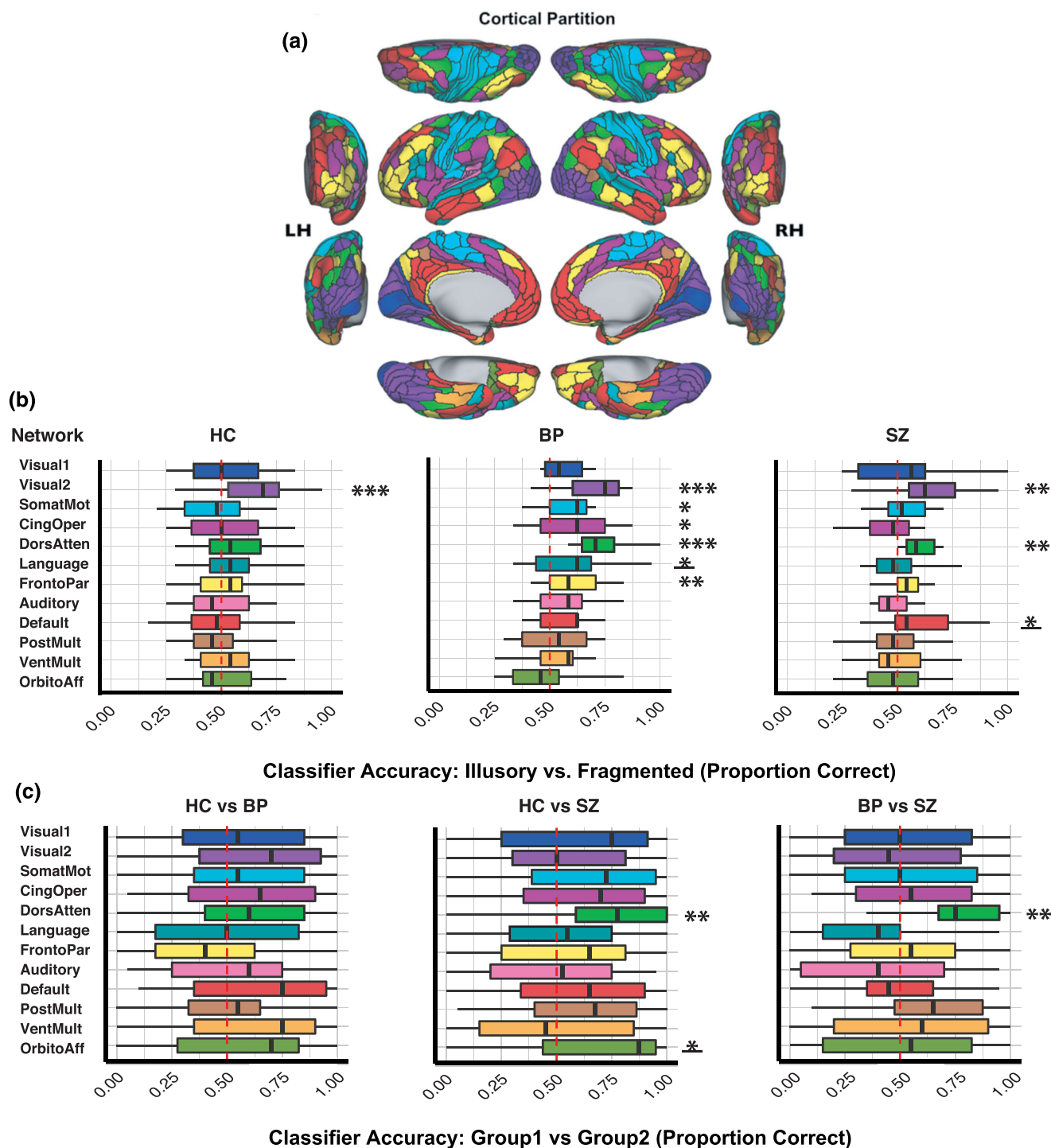


FIGURE 2 Cortical networks and multivariate pattern analysis (MVPA) results. (a) The 12 functional networks (Ji et al., 2019) are colour-coded to match panels (b) and (c). (b) Box plots depicting illusory/fragmented classification accuracy for each group using leave-two-runs-out cross-validation. The red dotted lines demarcate 50% performance. (c) Box plots depicting group classification accuracy for each pair of groups using repeated split-half cross-validation, where the features correspond to illusory/fragmented differences. See text for additional classification statistics. $*p_{corr} < .05$, $**p_{corr} < .01$, $***p_{corr} \leq .001$. All results could also pass a Bonferroni correction, except for the ones underlined.

calculated as the Euclidean distance of the head position in one frame as compared to the one preceding. One HC and one BP did not perform a resting-state scan; one SZ

and one BP had too few frames after motion scrubbing (<2.5 standard deviations relative to the mean of their respective subject groups). Group comparisons on the

remaining subjects (19 HCs, 15 SZs and 13 BPs) revealed no differences on either the mean framewise displacement after motion scrubbing ($M_{HC} = .12$, $M_{BP} = .15$ and $M_{SZ} = .14$ mm; $F[2,44] = 1.49$, $p = .23$) or the mean number of unscrubbed frames (HC—696, BP—632, SZ—663; $F[2,44] = 1.59$, $p = .22$).

For the task scans, there were six task regressors, one for each instructional screen (illusory/fragmented) and one for each of the four trial types (illusory/fragmented, easy/hard). As in our past study (Keane, Barch, et al., 2021), regressors were included for the instructional screens since each involved a change in perceptual set that did not occur elsewhere in the experiment. A standard fMRI general linear model (GLM) was fit to task-evoked activity convolved with the SPM canonical hemodynamic response function (using the function `spm_hrf.m`). Betas for the illusory and fragmented condition were derived from all trials of the relevant condition across all four runs. For the within-group classifier analyses, described below, task activation betas were derived separately for each run, but all other steps were the same as described.

The location and role of each parcel was considered within the context of their functional network affiliations. As noted, an advantage of an analysis based on networks (rather than individual clusters) is that it substantially increases power to detect average-size effects (Noble et al., 2022). We used the Cole-Anticevic Brain Network partition, which comprised 12 functional networks that were constructed from the above-mentioned parcels and that were defined via a General Louvain community detection algorithm using resting-state data from 337 healthy adults (Ji et al., 2019) (Figure 2a). This partition included: well-known sensory networks—primary visual, secondary visual, auditory, somatosensory; previously identified cognitive networks—fronto-parietal, dorsal attention, cingulo-opercular, and default mode; a left-lateralized language network; and three entirely novel networks—posterior multimodal, ventral multimodal and orbito-affective.

2.3.4 | Multivariate pattern analyses

To understand whether specific networks were being used within each subject group, we averaged the parcel-wise betas across the two difficulty levels in each condition and performed an MVPA with an exhaustive leave-two-runs-out cross-validation for each network (equivalent to split-half cross-validation). This procedure, which has been implemented before (Keane, Barch, et al., 2021), was applied to each subject individually. The procedure entailed determining, for each network,

whether the illusory and fragmented parcel-wise betas for each of the two left-out runs better correlated to the illusory or fragmented betas averaged across the remaining runs (with the number of illusory/fragmented trials always being the same in each run). Thus, the features corresponded to the betas for each condition (e.g., 23 beta values per condition per run for the 23 parcels of the DAN), the labels were ‘illusory’ or ‘fragmented’, and the possible score for a left-out run could be 0, .5 or 1.0, depending on whether one or both conditions were properly classified. Similar to past studies, we chose Pearson correlation as the minimum distance classifier (Mill et al., 2020; Mur et al., 2009; Spronk et al., 2020) because it intuitively measures a group’s proximity to an individual in multivariate feature space without requiring parameter choices (e.g., the ‘C’ parameter in support vector machines). Note that this distance metric, being correlational, was insensitive to potential differences between the mean activation value of the illusory and fragmented conditions for a given network. Note also that simple linear classifiers perform just as well as sophisticated non-linear methods (e.g., deep learning) with noisy (fMRI) data (Schulz et al., 2020). Results were averaged for each subject across the six possible ways to divide the four runs between test and validation. Statistical significance was determined via permutation tests, which generated a null distribution of classification accuracies through the same procedure with 10,000 samples. That is, for each sample and before the cross-validation, the ‘illusory’ and ‘fragmented’ labels were shuffled for each subject and run. The classification results were then averaged across subjects and across the six possible divisions of test and validation data sets. False Discovery Rate (FDR) correction was applied to the 12 tests (one for each resting-state network). As a more rigorous test, we also reported the tests that could survive a Bonferroni correction across the 12 networks ($\alpha = .0042$).

To determine which networks were differentially modulated between groups, we conducted, for each pair of groups, a repeated split-half cross-validation using illusory/fragmented activation differences as features (also referred to as ‘modulations’) and group membership as labels. A variant of this procedure has been used in past clinical studies (Mill et al., 2020) and so was expected to provide additional insights in SZ. For each repetition of the cross-validation, we considered whether the parcel-wise activation differences (illusory-fragmented) for half of the subjects better correlated with the averaged activation differences of the remaining subjects for each of the two subject groups. As before, this classifier, being correlational, was not sensitive to group differences in a network’s mean modulation value; it was instead sensitive to whether a subject’s vectorized activity pattern across

network parcels better correlated to the averaged vectorized pattern of a particular group. Folds were stratified to ensure that each was representative of the overall sample. Results were averaged over 20 repetitions, by which point statistical power plausibly reaches a near-maximum (Valente et al., 2021). Accuracy, sensitivity, specificity and areas under the curve were calculated using classification values that were averaged across repetitions for each subject. The classifier's statistical significance was judged relative to a null distribution, which was created by shuffling the subject group labels and repeating the foregoing steps for each of 10,000 samples. Note that the labels were permuted outside of the cross-validation loops, which gives less optimistic (and more realistic) estimates of the underlying null (Etzel & Braver, 2013; Valente et al., 2021). Note also that for each group comparison and across all networks, the mean value of the null distribution always fell near 50% accuracy (range: 49.9%–51.2%), demonstrating that sample size imbalances introduced minimal classifier bias. MVPAs were applied to each of the 12 resting-state networks and resulting *p*-values were FDR corrected as before. As above, as a more conservative test, we also considered which results could survive a Bonferroni correction ($\alpha = .0042$). In all of the MVPAs, the networks that were of special interest were those associated with cognitive control (frontoparietal, dorsal attention, default mode, cingulo-opercular) and visual perceptual organization (secondary visual network) (see Section 1).

2.3.5 | Estimating resting-state functional connectivity (RSFC) matrices

For each group, we generated a resting-state functional connectivity (RSFC) matrix to model shape completion via activity flow mapping (see below). We derived each subject's RSFC by using principal components regression with 100 components, as in past studies (Hearne et al., 2021; Keane, Barch, et al., 2021). PC regression was preferred over ordinary least squares to prevent overfitting (using all components would inevitably capture noise in the data). Multiple regression was preferred over Pearson correlation since the former removes indirect connections (Reid et al., 2019). For example, if there exists a true connection from A to B and B to C, a Pearson correlation, but not regression, would incorrectly show connections between A and C. To generate a subject's RSFC, for each target parcel time series, we used PCA to decompose the time series of the remaining ($N = 359$) parcels into 100 components, regressed the target onto the PCA scores, and back-transformed the PCA betas into a parcel-wise vector. The average amount of

variance explained by the components across subjects was 84% for controls [range: 81%–88%], 84% for bipolar patients [range: 78%–89%], and 83% for SZ patients [range: 81%–85%].

2.3.6 | Brain activity flow mapping ('ActFlow')

In the next set of analyses, we employed RSFC matrices and brain activity flow mapping to model illusory/fragmented task activation differences. For each subject, task activations in a held-out parcel was predicted as the weighted average of the activations of all other parcels, with the weights being given by the resting-state connections (for formal and graphical depiction see Figure S1). The accuracy of the activity flow predictions was then assessed by computing the overlap (Pearson correlation) between the predicted and actual task activations. Subject-level overlap was expressed by comparing actual and predicted activations for each subject, and then averaging the resulting Fisher-transformed *r* values (r_z) across subjects. Statistical significance was determined by comparing the vector of r_z values to zero via a one-sample *t* test. Note that ActFlow has yielded accurate estimates of task-evoked activations for cognitive control, visual working memory, and visual shape completion tasks, among others (Cole et al., 2016; Hearne et al., 2021; Keane, Barch, et al., 2021).

We applied the ActFlow methodology to consider possible group differences in how other networks interfaced with the secondary visual network. The secondary visual network was of interest because it is central to shape completion in healthy adults (Keane, Barch, et al., 2021) and because particular regions falling within this network (i.e., LO, V4) have been repeatedly implicated in shape completion via EEG, MEG, TMS, and single-unit recording (Cox et al., 2013; Halgren et al., 2003; Murray et al., 2006; Wokke et al., 2013). We considered how ActFlow estimates improved in that network, when any of the remaining networks were individually added (Figure 3). This change was determined simply by comparing via a paired *t*-test the prediction accuracies (Fisher *Z*-transformed correlations) before and after adding each network. A significant improvement would indicate which other networks, if any, guided activity flow in the secondary visual network. Note that we chose this method for assessing top-down connectivity since our method for computing RSFC removes indirect connections and has been used in many past studies to model activity associated with cognition and perception, as noted above (Cole et al., 2016; Hearne et al., 2021; Keane, Barch, et al., 2021; Mill et al., 2020), and since our

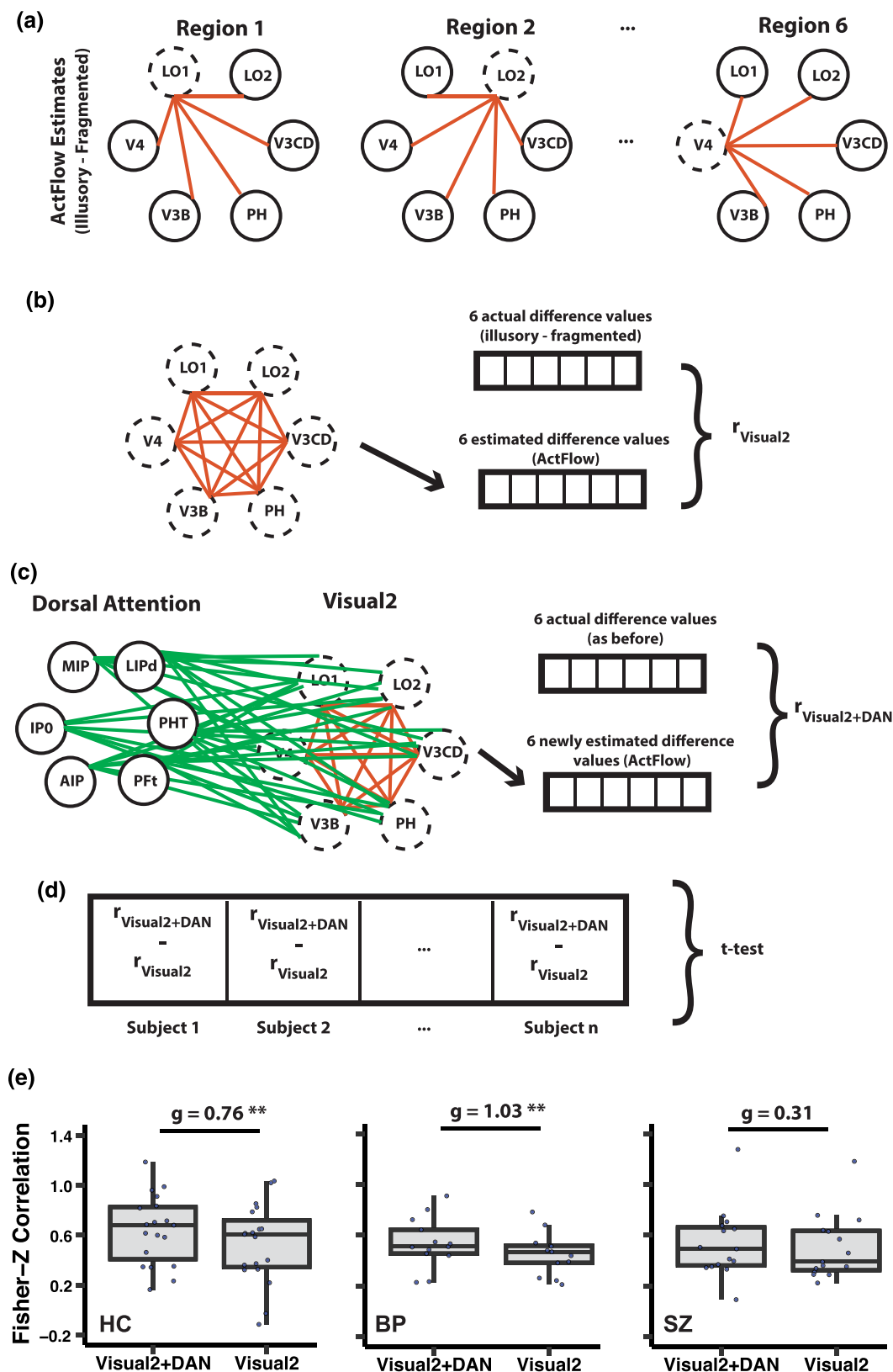


FIGURE 3 Legend on next page.

FIGURE 3 Modelling contributions of the dorsal attention network (DAN) to the secondary visual network (Visual2). (a) For a given subject, illusory/fragmented task activation differences ('modulations') for each Visual2 parcel was estimated (dotted circles) using actual task modulations in the remaining parcels (solid circles) and their resting-state connections (red lines). For illustration, only six regions are shown for each network. (b) Modelling accuracy was defined as the correlation between actual and estimated task modulations, across the Visual2 parcels. (c) Task modulations were again estimated via ActFlow, except that, this time, the connections and modulations from dorsal attention regions could also contribute. (d) The original and re-calculated estimates for each group were compared (after a Fisher Z transform) via a paired *t* test. (e) As shown in the boxplots, the DAN could significantly improve ActFlow modelling estimates in the secondary visual network in controls and bipolar patients, but not in schizophrenia patients. (Note that removing the one SZ outlier further reduced the improvement in that group—see text.) $**p < .01$. Figure is adapted from Keane, Barch, et al. (2021).

goal was not to choose between models with multiple nodes (as with dynamic causal modelling) but instead to simply evaluate the integrity of a single channel of connections between two networks within each group.

2.3.7 | Predicting cognitive disorganization from illusory/fragmented parcel-wise modulations

The DAN was differentially modulated in SZs relative to the other groups, and cognitive disorganization has been associated with impaired shape completion and altered neural oscillations (Keane et al., 2019; Spencer et al., 2004; Spencer & Ghorashi, 2014). Can these results be linked more directly? To consider the question, we ran a linear regression with leave-one-out cross-validation. Leave-one-out was chosen because, contrary to popular conceptions, it generally yields the least bias/variance for prediction (Zhang & Yang, 2015) and because its predictions can generalize surprisingly well to held-out fMRI data (Anticevic et al., 2014; Rosenberg et al., 2015). Within each training loop, the outcome variable (disorganization as assessed with the PANSS) and each predictor variable (modulations for a given DAN parcel) were z-scored using the means and standard deviations from the training set (to prevent circularity) (Mill et al., 2020; Shen et al., 2017). In the training set, the disorganization scores were regressed onto the modulations and the resulting beta coefficients were used to predict the held-out subject's disorganization score. Model prediction accuracy was gauged as the mean absolute error between predicted and actual disorganization (MAE). We also report the correlation (Pearson's *r*) between actual disorganization values and those predicted by the model, as well as the coefficient of codetermination (R^2 , also referred to as 'predicted R^2 ' or *q*), which uses the sums-of-squares formulation (rather than the square of the correlation) and which corresponds to how much the outcome variable can be predicted in absolute terms (Scheinost et al., 2019). Statistical significance was judged via

permutation testing. That is, we compared the true MAE to a distribution of such values that were generated by randomly shuffling the disorganization scores across subjects (without changing the feature matrix). As before, the disorganization variable was reshuffled once for each of the 10,000 samples of the null distribution, before the cross-validation loops. To demonstrate robustness, we additionally ran repeated leave-two-out and 10-fold cross-validation. The method was the same as just described except that MAE was averaged across 100 randomized splits between test and training.

2.3.8 | Experimental design and statistical analysis

The neuroimaging results are described in four sections. In the first, we quantified each network's contribution to shape completion by applying MVPA to parcel-wise illusory and fragmented task activations. This analysis would reveal, for each group, the networks that encoded the illusory and fragmented conditions distinctly. As a more direct test, we then applied MVPA to parcel-wise task activation differences (illusory-fragmented) to determine which networks might encode shape completion uniquely in SZ patients compared to the other groups. If shape completion is carried out by way of higher-order cognitive networks in SZ, a cognitive control network should encode the illusory/fragmented difference and this network should distinguish SZ patients from the other two subject groups. In the third section, we considered whether dorsal attention network activity (whose relevance was established in the above analyses) could predict cognitive disorganization severity. In the fourth section, we determined which network contained the most informative resting-state connections for inferring differential task activity in the secondary visual network (whose relevance was established in Section 1) by using brain activity flow mapping. Brain activity flow mapping allowed us to determine whether the dorsal attention network (and other networks) could model activity in the

secondary visual network in each group, which in turn provided clues regarding how the groups might differ in the use of top-down feedback during shape completion.

Analyses were performed with RStudio (Version 1.2.1335) and MATLAB R2019a, except for the behavioral analyses which were done with SPSS version 27. Cortical visualizations were created with Workbench (version 1.2.3). The final sample sizes were determined by the duration of funding (see Acknowledgements and Section 2.1 above). False Discovery Rate correction, when applied, was denoted by p_{corr} and had a threshold of $q < .05$ (Benjamini & Hochberg, 1995). T test effect sizes were given as Hedges' g and were generated with the measures-of-effect-size toolbox in MATLAB (Hentschke, 2021).

3 | RESULTS

3.1 | Behavioral task performance

Employing a 2 (task condition) by 2 (difficulty) by 3 (group) within-subjects ANOVA (type III sum of squares), we found that performance was more accurate in the fragmented than illusory condition (88.9% versus 80.9%, $F[1,48] = 28.9$, $p < .01$) and better in the ('easy') large-rotation condition than the 'hard' small-rotation condition ($F[1,48] = 229.5$, $p < 10^{-19}$) (see Table 2). The accuracy difference between illusory and fragmented conditions did not depend on difficulty level, although there was a trend towards a greater difference on the smaller rotation condition (two-way interaction: $F[2,48] = 3.3$, $p = .08$). The marginal interaction probably arose from ceiling effects for the fragmented condition since there was no corresponding interaction in the reaction time data ($F[2,48] = .82$, $p = .37$). Reaction time data were in other ways entirely predictable from the accuracy results, with faster performance in the fragmented than the illusory condition ($F[1,48] = 11.4$, $p < .01$), and faster performance in the easy than the hard condition (F

$[1,48] = 65.7$, $p < 10^{-9}$). The no-response trials were infrequent, occurring on only 3.9% of the trials on average. The frequency of no-response trials did not vary with difficulty level or task condition nor was there an interaction between difficulty and task condition (all $p > .10$). Note that one SZ patient exhibited chance task performance but was retained so as to have a more typical and representative patient sample. Most importantly, across all three ANOVAs (accuracy, RT, no-response frequency), there were no main effects or interactions with subject group (all $p > .28$; all *partial eta squared* $< .055$). Note that we were not necessarily expecting significant behavioral differences with our sample sizes since the group difference in a larger-scale study was of medium-large magnitude ($d = .67$; 134 patients, 66 HCs) (Keane et al., 2019). We nevertheless propose reasons in the Discussion why our observed shape completion deficits were smaller than anticipated.

Consistent with past results (Keane et al., 2019; Keane, Barch, et al., 2021), the fragmented and illusory conditions were highly correlated behaviorally across subjects (accuracy— $r = .67$, $p < 10^{-7}$; RT— $r = .85$, $p < .10^{-11}$), confirming that the two were reliant upon a common core of mechanisms. The correlations were robust and remained significant when calculated with non-parametric tests or after log-transforming the RT data.

3.2 | Shape completion modulates the dorsal attention network in SZ and bipolar patients but not in healthy controls

To determine the networks relevant to shape completion in each group, we ran a leave-two-runs-out MVPA, which assessed—for each subject and network—whether the illusory and fragmented betas from the training runs could be used to correctly classify the illusory and fragmented betas from the two remaining runs. To determine the involvement of each network within a group, classification accuracy results were aggregated across subjects and compared to a null distribution (see Methods). For healthy controls, the secondary visual network encoded the modulations, as already reported (accuracy = 63%, $p_{corr} = .001$) (Keane, Barch, et al., 2021). For SZ patients, three networks encoded the modulations: secondary visual (accuracy = 63%, $p_{corr} = .002$), dorsal attention (accuracy = 61%, $p_{corr} = .008$), and default mode (accuracy = 59%, $p_{corr} < .05$). Finally, for bipolar patients, six significant networks encoded the modulations: secondary visual (accuracy = 69%, $p_{corr} < .0001$); somatomotor (accuracy = 59%, $p_{corr} = .03$), cingulo-opercular (accuracy = 60%, $p_{corr} = .01$), dorsal attention (accuracy = 71%, $p_{corr} < .0001$), language

TABLE 2 Task performance

	HC	BP	SZ
% Correct, Illus	82.9 (3.0)	80.0 (3.5)	79.6 (3.4)
% Correct, Frag	89.6 (2.2)	89.7 (2.5)	87.4 (2.4)
Reaction time (s), Illus	1.04 (.07)	.93 (.08)	1.06 (.07)
Reaction time (s), Frag	.94 (.07)	.84 (.08)	.99 (.08)
% Slow response, Illus	4.3 (2.6)	.4 (3.0)	5.2 (2.9)
% Slow response, Frag	6.8 (2.8)	.6 (3.2)	6.3 (3.1)

Note: Mean values for each variable (with standard error of the mean).

(accuracy = 59%, $p_{corr} = .03$) and frontoparietal (accuracy = 59%, $p_{corr} = .010$). Most of the foregoing results could also survive a Bonferroni correction (see Figure 2). These results suggest that whereas the secondary visual network was important in each patient group (essentially an out-of-sample replication of the control group result), the dorsal attention network was also relevant. Unexpectedly, these results also show that multivariate traces of shape completion were distributed through more networks in each patient group.

3.3 | Dorsal attention network activity distinguished people with and without schizophrenia

To consider whether groups could be distinguished in parcel-wise patterns, we trained MVPA classifiers separately for the 12 functional networks (Ji et al., 2019). For each pair of subject groups and for each network, the classifier used illusory/fragmented activation differences to categorize subjects by their group membership (see Methods). After FDR correction, no network could distinguish bipolar patients and healthy controls. The networks that could distinguish SZ patients from healthy controls were the dorsal attention ($p_{corr} = .005$, sensitivity_{SZ} = .74, specificity_{SZ} = .74, AUC = .86) and orbito-affective ($p_{corr} = .03$, sensitivity_{SZ} = .65, specificity_{SZ} = .72, AUC = .77). When comparing bipolar and SZ patients, only the DAN reached significance ($p_{corr} = .007$, sensitivity_{SZ} = .73, specificity_{SZ} = .73, AUC = .87). The primary and secondary visual networks did not distinguish any of the three groups (all $p_{corr} > .24$); this held true even without statistical correction (all $p > .06$). By contrast, both DAN results were robust and could also survive Bonferroni correction (both $p < .0007$). To summarize, patterns of dorsal attention task activations could distinguish SZ patients from the other groups. These results, which will be elaborated upon more fully in the Discussion, are consistent with our hypothesis that brain network differences during visual perceptual organization in SZ are primarily related to higher-level cognition.

3.4 | Dorsal attention network activity could predict cognitive disorganization

Increased cognitive disorganization has been associated with poorer shape completion and abnormal oscillations, as noted (Keane et al., 2019; Spencer et al., 2004; Spencer & Ghorashi, 2014). Task-related DAN modulations can distinguish SZ patients from the other subject groups (Figure 2c). Can these variables be linked more

directly? To consider the question, we individually regressed this clinical variable onto the modulations of the 23 dorsal attention parcels using leave-one-out cross-validation with permutation testing (see Methods). Across all 31 patients, the modulations were indeed related to cognitive disorganization ($R^2 = .12$, $r = .65$, $MAE = .78$, $p = .007$). These results would also be significant if we were to use leave-two-out or 10-fold cross-validation (both $p \leq .01$) or if we were to use raw (non-z-scored) data ($p < .01$; see Figure S2). To consider how specific these predictions were to cognitive disorganization, we repeated the above procedure for the remaining four PANSS symptom types (depressive, negative, positive and excitement). No other symptom type could be predicted with the dubious exception of excitement, which was not presaged by any previous study and which would not survive any type of correction for multiple comparisons ($R^2 = -.3$, $r = .51$, $MAE = 1.1$, $p = .04$; all other symptoms: $p > .31$ before correction).¹

3.5 | Potentially reduced feedback (but not feedforward) activity between the dorsal attention and secondary visual networks in schizophrenia

A recently-developed predictive modelling approach—activity flow mapping ('ActFlow') (Cole et al., 2016)—has demonstrated that resting-state connections are likely relevant to shape completion in healthy controls (Keane, Barch, et al., 2021). This method computes the activation difference (illusory minus fragmented) in a held-out 'target' parcel as the linear weighted sum of the activation differences in all other parcels, with the weights being given by the resting-state connections to the target (Figure S1). This algorithm is based on neural network simulations, and can thus be thought of as a rough simulation of the movement of task-evoked activity that likely contributed to each brain region's task-evoked activity level, which in turn can provide evidence that the resting-state connections mechanistically support shape completion. As described in more detail in the supporting information, when applied to all 360 parcels across cortex, the ActFlow modelling generated accurate results for all three groups (all $r > .56$, all $p < 10^{-6}$) and this accuracy did not differ between groups (all $p > .23$).

We developed a novel extension of the ActFlow framework, which shows that—in healthy controls—the DAN can model activity in the secondary visual network, potentially reflecting feedback to mid-level visual areas

¹We thank one of our manuscript reviewers for suggesting these additional analyses.

(Keane, Barch, et al., 2021). In this method, for each subject, we computed a single correlation between the actual and estimated parcel difference values (illusory-fragmented) across the 54 secondary visual network parcels. We then recomputed this correlation, when each of the 54 parcels could also be predicted by parcels and connections from the 23 dorsal attention regions (see Figure 3). Finally, we Fisher z -transformed the correlations, subtracted the two, and then performed a one-sample t test to see if the correlations increased as a result of the network's inclusion. As shown in Figure 3e, the DAN improved the predictions for the secondary visual network in healthy controls ($\Delta r \approx \Delta r_z = .11$; $t[18] = 3.3$, $p = .004$, $g = .76$) and bipolar patients ($\Delta r \approx \Delta r_z = .09$; $t[12] = 3.7$, $p = .003$, $g = 1.03$), but not in SZ patients ($\Delta r \approx \Delta r_z = .03$; $t[14] = 1.2$, $p = .25$, $g = .31$). There was one outlier in the SZ group (Figure 3e), but removing this subject would further diminish the effect size ($t[13] = .98$, $p = .35$, $g = .24$). No other network could model the secondary visual network in any group. These results would be the same with a Bonferroni correction (across all networks). Thus, the DAN fails to robustly model the secondary visual network in SZ, perhaps because of reduced feedback from dorsal attention to secondary visual areas.

An objection may be that the DAN failed to properly model the secondary visual network in the SZ group only because their parcels were less strongly connected to one another, irrespective of whether those connections were oriented bottom-up or top-down. To address this objection, we reversed the analysis and considered how Visual2 parcels might improve the modelling of the DAN parcels (see supporting information for graphical depiction). We found that adding Visual2 improved DAN modelling accuracy for the SZ group ($(\Delta r \approx \Delta r_z = .18$; $t[14] = 3.2$, $p = .006$, $g = .83$)), with somewhat smaller effects in the other groups (BP: $\Delta r \approx \Delta r_z = .11$; $t(12) = 1.8$, $p = .10$, $g = .49$; HC: $\Delta r \approx \Delta r_z = .11$; $t(18) = 2.5$, $p = .02$, $g = .56$) (Figure S3). Thus, feedforward processing from the secondary visual network seems to be intact in SZ, and there is no general problem in modelling a network in this group. To consider the relative contribution of feedforward and feedback activity between DAN and Visual2 within each group, we also determined whether the change in model accuracy (Δr_z) was greater in the feedforward versus the feedback ActFlow analysis. More exactly, we conducted paired t -tests and found that—in the SZ group—Visual2 improved the modelling of DAN more than DAN improved the modelling of Visual2 ($t[14] = 2.8$, $p = .01$, $g = .68$), consistent with a bias against top-down processing. The other groups exhibited no such bias (both $p > .76$, both $g < .1$).

4 | DISCUSSION

Visual shape completion plays a critical role in extracting object shape, size, position, and number from edge elements dispersed across the field of view. Prior electrophysiological and psychophysical work has suggested that SZ patients properly form illusory contours at initial stages of processing but potentially exhibit later-stage differences related to cognitive control. However, these findings have not been corroborated with other neuroscience methods and were generally limited by their lower spatial resolution. Here, we leveraged recent tools in computational neuroimaging to investigate the functional connections and brain networks that may differ in SZ during shape completion. We additionally considered whether such differences vary with cognitive disorganization, a cardinal feature of SZ. It was hypothesized that cognitive—but not visual—networks would be differentially active in SZ, that activity in one of these networks would be linked to cognitive disorganization, and, more speculatively, that top-down feedback to the secondary visual network would be faulty in SZ.

Five major findings emerged. First, the DAN was differentially active in SZ compared to the other groups. Next, the secondary visual network was strongly modulated within each group and did not differ group-wise in its activation pattern. Third, parcel-wise dorsal attention modulations across all patients could be used to predict cognitive disorganization severity. Fourth, in SZ, our modelling suggested little influence of the DAN on the secondary visual network (in contrast to the other groups, for which such an influence was observed), and strong influence of the secondary visual network on the DAN, although directionality will have to be confirmed with other approaches (see limitations below). A final unanticipated finding was that—regardless of diagnosis—patients incorporated more networks overall during shape completion. Below, we discuss these findings in more detail, identify potential limitations and suggest future directions along the way.

4.1 | Aberrant DAN activity in schizophrenia

Dorsal attention network activity was aberrant in SZ. This is consistent with earlier SZ studies, which have argued for abnormal dorsal stream contributions to motion perception (B. F. O'Donnell et al., 1996), stereopsis (Schechter et al., 2006) and fragmented object recognition (Sehatpour et al., 2010). Visual working memory deficits (and broader indices of cognition) have also been attributed to abnormal activation in posterior parietal

cortex (Hahn et al., 2018), which overlaps with the DAN. Others have also reported abnormal activation of the intraparietal sulcus (which also overlaps with dorsal attention network) during perceptual organization in SZ (Pokorny et al., 2021). A goal for future research will be to determine to what extent abnormal DAN activity emerges across these and other visual tasks in SZ. Because DAN differences were so large and because they were found relative to both healthy controls and bipolar disorder patients (AUCs > .85; sensitivities > .72; specificities > .72), such differences might yield a candidate biomarker for differential diagnosis or predicting future psychosis onset (Diamond et al., 2022). More highly powered studies with early-stage or high-risk patients are needed to confirm these possibilities.

DAN task activity was also related to cognitive disorganization but not any other symptom type after multiple comparison correction. The brain networks undergirding cognitive disorganization—alternatively referred to as ‘formal thought disorder’ or ‘conceptual disorganization’—are largely unknown perhaps because disorganization is less often parsed out as a separate construct (with many studies preferring instead to lump it in with the more encompassing positive symptom factor). An interesting possibility going forward will be to examine whether DAN activity during perceptual organization can serve as a proxy for cognitive disorganization or whether stimulating parts of DAN can ameliorate symptom severity.

4.2 | Evidence for reduced top-down attentional feedback in schizophrenia

It is not possible to tease apart feedforward and feedback activity using the hemodynamic response. However, a realistic possibility is that DAN dysfunction may disrupt top-down attentional amplification (Berkovitch et al., 2017; Berkovitch et al., 2018), which may be needed to properly notice and use illusory contours for shape discrimination (Keane et al., 2012). Such disruption has been linked specifically to cognitive disorganization, NMDA receptor hypofunction, and gamma band synchrony abnormalities, all of which characterize the SZ phenotype (Berkovitch et al., 2017). Others have also argued that unstable bottom-up signals from the visual periphery can over time lead to inappropriate models for top-down prediction (Adámek et al., 2022). This view fits with past behavioral work showing that SZ patients have impaired top-down attentional control for noticing subtle stimuli (Gold et al., 2007; Luck & Gold, 2008) and that there is impaired dorsal top-down feedback to ventral object-recognition areas (Tapia & Breitmeyer, 2011).

In light of the significant DAN activity in the SZ group, we speculate that patients may compensate for poor top-down modulation by carrying out computations within the DAN itself or by the DAN interfacing with other non-visual networks. This view of perceptual organization as being more cognitively reliant might also explain why conceptual knowledge aids interpretation of a vague visual stimulus more for people with subthreshold psychotic symptoms than for people without such symptoms (Teufel et al., 2015).

The above sketch implies that perceptual organization deficits may become more prominent if the (longer-latency) cognitive networks are given less time to operate (Wyatte et al., 2014). The current study presented a 250-ms pac-man configuration with no mask (to ensure a more robust BOLD response), but earlier psychophysical studies presented the pac-men for 200 ms with a mask 50 ms afterwards (Keane et al., 2019; Keane, Erlikhman, et al., 2021). This difference may help explain why the group effect on shape completion in a prior larger-scale study was medium-to-large ($d = .67$) (Keane et al., 2019), whereas the group difference in the current study was small ($d = .10$). Note that poor shape completion cannot purely be a masking effect because otherwise it would equally affect performance in the control ‘fragmented’ condition and because masking abnormalities in SZ are usually elicited with much shorter presentation durations (<100 ms) (Green et al., 2011). Instead, we suggest that higher-level access to such stimuli may be more important for patients and that a mask may limit this access. A prediction is that if we were to present stimuli more briefly with shorter masking SOAs or with more disruptive masks, then shape completion deficits should emerge more clearly. Another prediction is that applying single-pulse transcranial magnetic stimulation over dorsal attention regions between, say, 200–300 ms after stimulus onset (Wyatte et al., 2014) may elicit stronger shape completion impairments in SZ than in healthy or clinical controls.

4.3 | Bipolar disorder and schizophrenia have more diffuse neural representations

An unexpected but interesting finding was that completed shapes were encoded across a broader range of networks in each disorder. The reason is unknown but could be because computations ordinarily performed by vision could have been outsourced to nominally non-visual networks as suggested above; or this could be a byproduct of a less modularized brain network architecture (Ma et al., 2020). Networks in bipolar disorder may be especially less well-integrated and less centralized as

compared to those in healthy controls or even SZ (van Dellen et al., 2020). It is worth considering in future research whether similarly diffuse neural representational patterns emerge in other visual and cognitive tasks.

4.4 | Limitations and future directions

The most obvious limitation was sample size. However, we restricted our analyses to only 12 pre-defined networks for within-group and between-group comparisons. Network-based analyses are also plausibly more powerful in that they pool weaker parcel-wise effects over larger functionally related areas (Cremers et al., 2017; Ji et al., 2019; Noble et al., 2022). Moreover, the implicated networks in our analysis were suspected on the basis of past psychophysical and electrophysiological work (see Introduction). Additionally, the abnormal DAN activity in SZ was shown relative to two clinically and demographically well-matched groups (Table 1); both effects were large and could survive Bonferroni correction. Finally, the cognitive disorganization prediction was anticipated from past work (Keane et al., 2019; Spencer et al., 2004; Spencer & Ghorashi, 2014) and was shown with multiple forms of cross-validation and permutation testing using the larger combined patient sample ($n = 31$). Note that the length and number of runs was also unlikely a problem since, in each subject group, the MVPAs could unambiguously show the relevance of the secondary visual network and since task activity across cortex could be modeled with high accuracy (see supporting information) (Keane, Barch, et al., 2021). Notwithstanding the above considerations, including more subjects could reveal additional between-group network differences or relationships between DAN modulations and behavioral performance (which exploratory analyses failed to identify in any of the three groups). A larger sample could also provide the power to model (e.g., via DCM or psychophysiological interactions) whether specific visual connections during fragmented object perception may be aberrant in SZ, as reported by others (Pokorny et al., 2021).

Another limitation is that patients were on medication. Note, however, that the patient groups did not significantly differ on olanzapine equivalents and prior behavioral and electrophysiological studies found no relationships between shape completion and the type/dose of neuroleptics (Foxy et al., 2005; Keane et al., 2019; Spencer & Ghorashi, 2014).

It may also be objected that groups could have differed in their eye movements and this may have confounded the results. This is not problematic, however,

since (1) pac-men locations were equidistant from fixation, equally informative within a trial and matched between conditions, reducing the chance of systematic task condition differences; (2) the illusory and fragmented conditions were highly correlated in RT and accuracy and groups were undifferentiated on RT and accuracy, suggesting again that any possible eye movement differences impacted performance minimally; (3) saccading after stimulus onset would offer little benefit since saccade latency is ~ 200 ms (Sumner, 2011) and the stimuli appeared for only 250 ms at unpredictable times during a block (see also Keane, Barch, et al., 2021); (4) there is little evidence that eye movements impact visual shape completion in non-translating displays and some evidence that it has no effect relative to a control 'fragmented' condition (Cox et al., 2013; see the fixational heat maps in their Figure S2). A related objection is that subjects covertly attended to—and responded on the basis of—exactly one pac-man. Aside from being contrary to task demands, this again is unlikely since it is doubtful that any one network would be differentially modulated in such a scenario. The fact that the secondary visual network could strongly differentiate the two conditions, consistent with past research (Keane, Barch, et al., 2021), suggests that each group completed shapes in one condition but not in the other. Nevertheless, it could be useful to monitor eye movements in future studies of shape completion.

There could also be residual confounds: the Glasser atlas could have been inappropriate for patient groups (e.g., due to differences in cortical folding), lithium intake could have made the neural results incommensurable, or imperfect motion correction could have still led to group differences. However, RSFC matrices were similar between groups on univariate, multivariate, and Mantel tests, arguing against such confounds (see Figure S4).

To summarize, employing a well-validated perceptual organization task, we revealed clinically relevant DAN abnormalities in SZ, and more distributed shape representations across all patients, potentially reflecting compensatory mechanisms. Goals for future research will be to establish a causal role for the DAN and to consider whether briefer stimulus presentations can minimize potential compensatory cognitive influence or generate more obvious group differences in shape completion performance.

ACKNOWLEDGEMENTS

We thank Rebekah Boy, Laura Crespo, Lisa Cruz, Blair Singer and Dillon Smith for help in recruiting participants and collecting and organizing study data. We are also indebted to Michael Harms for assistance in finalizing the pulse sequence, Pamela Butler for assistance in

patient recruitment, and Takuya Ito and Carrisa Cocuzza for providing sample code. The authors additionally acknowledge the Office of Advanced Research Computing (OARC) at Rutgers University for providing access to the Amarel cluster and associated research computing resources (<http://oarc.rutgers.edu>). This work was supported by a National Institute of Mental Health Mentored Career Development Award (K01MH108783) to BPK.

CONFLICT OF INTEREST

The authors declare no competing conflicts of interest.

AUTHOR CONTRIBUTIONS

Conceptualization—BPK, DMB and MWC; data acquisition—BPK, MRS and JLT; formal analysis—BPK, RDM, MWC and DMB; funding acquisition—BPK; resources—MWC, BK and SMS; software—RDM, MWC and BPK; supervision—MWC, DMB, SMS and BK; visualization—BPK, RDM and MWC; first draft—BPK; review and editing—BPK, RDM, MWC, DMB, BK, SMS, MRS and JLT.

PEER REVIEW

The peer review history for this article is available at <https://publons.com/publon/10.1111/ejn.15889>.

DATA AVAILABILITY STATEMENT

Brain activity flow mapping MATLAB code is part of the freely-available ActFlow toolbox: <https://github.com/ColeLab/ActflowToolbox>. HCP minimal preprocessing pipelines may be found here: <https://github.com/Washington-University/HCPpipelines/releases>. The Cole Anticevic Brain Network partition can be found here: <https://github.com/ColeLab/ColeAnticevicNetPartition>. Neural data will be released within 12 months on OpenNeuro.org along with resting-state functional connectivity matrices and unthresholded task activation maps.

ORCID

Brian P. Keane  <https://orcid.org/0000-0002-7011-3380>

REFERENCES

- Adámek, P., Langová, V., & Horáček, J. (2022). Early-stage visual perception impairment in schizophrenia, bottom-up and back again. *Schizophrenia*, 8(1), 27–12. <https://doi.org/10.1038/s41537-022-00237-9>
- Addington, D., Addington, J., & Maticka-Tyndale, E. (1993). Assessing depression in schizophrenia: The Calgary Depression Scale. *The British Journal of Psychiatry*, 163(22), 39–44. <https://doi.org/10.1192/S0007125000292581>
- Anticevic, A., Cole, M. W., Repovs, G., Murray, J. D., Brumbaugh, M. S., Winkler, A. M., Savic, A., Krystal, J. H., Pearlson, G. D., & Glahn, D. C. (2014). Characterizing thalamo-cortical disturbances in schizophrenia and bipolar illness. *Cerebral Cortex*, 24(12), 3116–3130. <https://doi.org/10.1093/cercor/bht165>
- Beck, J. (1966). Effect of orientation and of shape similarity on perceptual grouping. *Perception & Psychophysics*, 1, 300–302. <https://doi.org/10.3758/BF03207395>
- Benjamini, Y., & Hochberg, J. (1995). Controlling the false discovery rate: A practical and powerful approach to multiple testing. *Journal of the Royal Statistical Society Series B-Methodological*, 57(1), 289–300. <https://doi.org/10.1111/j.2517-6161.1995.tb02031.x>
- Berkovitch, L., Dehaene, S., & Gaillard, R. (2017). Disruption of conscious access in schizophrenia. *Trends in Cognitive Sciences*, 21(11), 878–892. <https://doi.org/10.1016/j.tics.2017.08.006>
- Berkovitch, L., Del Cul, A., Maheu, M., & Dehaene, S. (2018). Impaired conscious access and abnormal attentional amplification in schizophrenia. *NeuroImage. Clinical*, 18, 835–848. <https://doi.org/10.1016/j.nicl.2018.03.010>
- Bollini, P., Pampallona, S., Tibaldi, G., Kupelnick, B., & Munizza, C. (1999). Effectiveness of antidepressants—Meta-analysis of dose-effect relationships in randomised clinical trials. *The British Journal of Psychiatry: The Journal of Mental Science*, 174, 297–303. <https://doi.org/10.1192/bjp.174.4.297>
- Bunney, W. E., Hetrick, W. P., Bunney, B. G., Patterson, J. V., Jin, Y., Potkin, S. G., & Sandman, C. A. (1999). Structured Interview for Assessing Perceptual Anomalies (SIAPA). *Schizophrenia Bulletin*, 25(3), 577–592. <https://doi.org/10.1093/oxfordjournals.schbul.a033402>
- Canivez, G. L., & Watkins, M. W. (2010). Investigation of the factor structure of the Wechsler adult intelligence scale—Fourth edition (WAIS-IV): Exploratory and higher order factor analyses. *Psychological Assessment*, 22(4), 827–836. <https://doi.org/10.1037/a0020429>
- Cannon-Spoor, H. E., Potkin, S. G., & Wyatt, R. J. (1982). Measurement of premorbid adjustment in chronic schizophrenia. *Schizophrenia Bulletin*, 8(3), 470–484. <https://doi.org/10.1093/schbul/8.3.470>
- Cassidy, F., Ahearn, E. P., & Carroll, B. J. (2001). Substance abuse in bipolar disorder. *Bipolar Disorders*, 3(4), 181–188. <https://doi.org/10.1034/j.1399-5618.2001.30403.x>
- Chen, S., Weidner, R., Zeng, H., Fink, G. R., Müller, H. J., & Conci, M. (2020). Tracking the completion of parts into whole objects: Retinotopic activation in response to illusory figures in the lateral occipital complex. *NeuroImage*, 207, 116426. <https://doi.org/10.1016/j.neuroimage.2019.116426>
- Ciric, R., Wolf, D. H., Power, J. D., Roalf, D. R., Baum, G. L., Ruparel, K., Shinohara, R. T., Elliott, M. A., Eickhoff, S. B., Davatzikos, C., Gur, R. C., Gur, R. E., Bassett, D. S., & Satterthwaite, T. D. (2017). Benchmarking of participant-level confound regression strategies for the control of motion artifact in studies of functional connectivity. *NeuroImage*, 154, 174–187. <https://doi.org/10.1016/j.neuroimage.2017.03.020>
- Cole, M. W., Bassett, D. S., Power, J. D., Braver, T. S., & Petersen, S. E. (2014). Intrinsic and task-evoked network architectures of the human brain. *Neuron*, 83(1), 238–251. <https://doi.org/10.1016/j.neuron.2014.05.014>
- Cole, M. W., Ito, T., Bassett, D. S., & Schultz, D. H. (2016). Activity flow over resting-state networks shapes cognitive task activations. *Nature Neuroscience*, 19(12), 1718–1726. <https://doi.org/10.1038/nn.4406>

- Cox, M. A., Schmid, M. C., Peters, A. J., Saunders, R. C., Leopold, D. A., & Maier, A. (2013). Receptive field focus of visual area V4 neurons determines responses to illusory surfaces. *Proceedings of the National Academy of Sciences of the United States of America*, 110(42), 17095–17100. <https://doi.org/10.1073/pnas.1310806110/-/DCSupplemental>
- Cremers, H. R., Wager, T. D., & Yarkoni, T. (2017). The relation between statistical power and inference in fMRI. *PLoS ONE*, 12(11), e0184923. <https://doi.org/10.1371/journal.pone.0184923>
- Diamond, A., Silverstein, S. M., & Keane, B. P. (2022). Visual system assessment for predicting a transition to psychosis. *Translational Psychiatry*, 12, 351–359. <https://doi.org/10.1038/s41398-022-0211>
- Dima, D., Dietrich, D. E., Dillo, W., & Emrich, H. M. (2010). Impaired top-down processes in schizophrenia: A DCM study of ERPs. *NeuroImage*, 52(3), 824–832. <https://doi.org/10.1016/j.neuroimage.2009.12.086>
- Dixon, L. (1999). Dual diagnosis of substance abuse in schizophrenia: Prevalence and impact on outcomes. *Schizophrenia Research*, 35(Suppl), S93–S100. [https://doi.org/10.1016/S0920-9964\(98\)00161-3](https://doi.org/10.1016/S0920-9964(98)00161-3)
- Dunayevich, E., & Keck, P. E. (2000). Prevalence and description of psychotic features in bipolar mania. *Current Psychiatry Reports*, 2(4), 286–290. <https://doi.org/10.1007/s11920-000-0069-4>
- Etzel, J. A., & Braver, T. S. (2013). MVPA permutation schemes: Permutation testing in the land of cross-validation (pp. 140–143). Presented at the Proceedings - 2013 3rd International Workshop on Pattern Recognition in Neuroimaging, PRNI 2013. <https://doi.org/10.1109/PRNI.2013.44>
- Foxe, J. J., Murray, M. M., & Javitt, D. C. (2005). Filling-in in schizophrenia: A high-density electrical mapping and source-analysis investigation of illusory contour processing. *Cerebral Cortex (New York, NY: 1991)*, 15(12), 1914–1927. <https://doi.org/10.1093/cercor/bhi069>
- Gardner, D. M., Murphy, A. L., O'Donnell, H., Centorrino, F., & Baldessarini, R. J. (2010). International consensus study of anti-psychotic dosing. *The American Journal of Psychiatry*, 167(6), 686–693. <https://doi.org/10.1176/appi.ajp.2009.09060802>
- Glasser, M. F., Coalson, T. S., Robinson, E. C., Hacker, C. D., Harwell, J., Yacoub, E., Ugurbil, K., Andersson, J., Beckmann, C. F., Jenkinson, M., Smith, S. M., & van Essen, D. C. (2016). A multi-modal parcellation of human cerebral cortex. *Nature*, 536(7615), 171–178. <https://doi.org/10.1038/nature18933>
- Glasser, M. F., Sotiropoulos, S. N., Wilson, J. A., Coalson, T. S., Fischl, B., Andersson, J. L., Xu, J., Jbabdi, S., Webster, M., Polimeni, J. R., van Essen, D., Jenkinson, M., & WU-Minn HCP Consortium. (2013). The minimal preprocessing pipelines for the human connectome project. *NeuroImage*, 80(C), 105–124. <https://doi.org/10.1016/j.neuroimage.2013.04.127>
- Gold, J. M., Fuller, R. L., Robinson, B. M., Braun, E. L., & Luck, S. J. (2007). Impaired top-down control of visual search in schizophrenia. *Schizophrenia Research*, 94(1–3), 148–155. <https://doi.org/10.1016/j.schres.2007.04.023>
- Green, M. F., Lee, J., Wynn, J. K., & Mathis, K. I. (2011). Visual masking in schizophrenia: Overview and theoretical implications. *Schizophrenia Bulletin*, 37(4), 700–708. <https://doi.org/10.1093/schbul/sbr051>
- Grzeczowski, L., Clarke, A. M., Francis, G., Mast, F. W., & Herzog, M. H. (2017). About individual differences in vision. *Vision Research*, 141, 282–292. <https://doi.org/10.1016/j.visres.2016.10.006>
- Hahn, B., Robinson, B. M., Leonard, C. J., Luck, S. J., & Gold, J. M. (2018). Posterior parietal cortex dysfunction is central to working memory storage and broad cognitive deficits in schizophrenia. *Journal of Neuroscience*, 38(39), 8378–8387. <https://doi.org/10.1523/JNEUROSCI.0913-18.2018>
- Halgren, E., Mendola, J., Chong, C. D. R., & Dale, A. M. (2003). Cortical activation to illusory shapes as measured with magnetoencephalography. *NeuroImage*, 18(4), 1001–1009. [https://doi.org/10.1016/S1053-8119\(03\)00045-4](https://doi.org/10.1016/S1053-8119(03)00045-4)
- Hearne, L. J., Mill, R. D., Keane, B. P., Repovs, G., Anticevic, A., & Cole, M. W. (2021). Activity flow underlying abnormalities in brain activations and cognition in schizophrenia. *Science Advances*, 7(29). <https://doi.org/10.1126/sciadv.abf2513>
- Heatherston, T. F., Kozlowski, L. T., Frecker, R. C., & Fagerstrom, K. O. (1991). The Fagerstrom test for nicotine dependence - a revision of the Fagerstrom tolerance questionnaire. *British Journal of Addiction*, 86(9), 1119–1127. <https://doi.org/10.1111/j.1360-0443.1991.tb01879.x>
- Hentschke, H. (2021). hhentschke/measures-of-effect-size-toolbox (<https://github.com/hhentschke/measures-of-effect-size-toolbox>). *GitHub*.
- Ji, J. L., Spronk, M., Kulkarni, K., Repovs, G., Anticevic, A., & Cole, M. W. (2019). Mapping the human brain's cortical-subcortical functional network organization. *NeuroImage*, 185, 35–57. <https://doi.org/10.1016/j.neuroimage.2018.10.006>
- Kay, S. R., Fiszbein, A., & Opler, L. A. (1987). The positive and negative syndrome scale (PANSS) for schizophrenia. *Schizophrenia Bulletin*, 13(2), 261–276. <https://doi.org/10.1093/schbul/13.2.261>
- Keane, B. P. (2018). Contour interpolation: A case study in modularity of mind. *Cognition*, 174, 1–18. <https://doi.org/10.1016/j.cognition.2018.01.008>
- Keane, B. P., Barch, D. M., Mill, R. D., Silverstein, S. M., Krekelberg, B., & Cole, M. W. (2021). Brain network mechanisms of visual shape completion. *NeuroImage*, 236, 118069. <https://doi.org/10.1016/j.neuroimage.2021.118069>
- Keane, B. P., Erlikhman, G., Serody, M. R., & Silverstein, S. M. (2021). A brief psychometric test reveals robust shape completion deficits in schizophrenia that are less severe in bipolar disorder. *Schizophrenia Research*, 240, 78–80. <https://doi.org/10.1016/j.schres.2021.12.015>
- Keane, B. P., Joseph, J., & Silverstein, S. M. (2014). Late, not early, stages of Kanizsa shape perception are compromised in schizophrenia. *Neuropsychologia*, 56, 302–311. <https://doi.org/10.1016/j.neuropsychologia.2014.02.001>
- Keane, B. P., Lu, H., Papathomas, T. V., Silverstein, S. M., & Kellman, P. J. (2012). Is interpolation cognitively encapsulated? Measuring the effects of belief on Kanizsa shape discrimination and illusory contour formation. *Cognition*, 123(3), 404–418. <https://doi.org/10.1016/j.cognition.2012.02.004>
- Keane, B. P., Paterno, D., Kastner, S., Krekelberg, B., & Silverstein, S. M. (2019). Intact illusory contour formation but equivalently impaired visual shape completion in first- and later-episode schizophrenia. *Journal of Abnormal Psychology*, 128(1), 57–68. <https://doi.org/10.1037/abn0000384>

- Kellman, P. J., & Shipley, T. (1991). A theory of visual interpolation in object perception. *Cognitive Psychology*, 23(2), 141–221. [https://doi.org/10.1016/0010-0285\(91\)90009-D](https://doi.org/10.1016/0010-0285(91)90009-D)
- Keshavan, M. S., Morris, D. W., Sweeney, J. A., Pearlson, G., Thaker, G., Seidman, L. J., Eack, S. M., & Tamminga, C. (2011). A dimensional approach to the psychosis spectrum between bipolar disorder and schizophrenia: The Schizo-Bipolar Scale. *Schizophrenia Research*, 133(1–3), 250–254. <https://doi.org/10.1016/j.schres.2011.09.005>
- Lichtenstein, P., Yip, B. H., Björk, C., Pawitan, Y., Cannon, T. D., Sullivan, P. F., & Hultman, C. M. (2009). Common genetic determinants of schizophrenia and bipolar disorder in Swedish families: A population-based study. *Lancet*, 373(9659), 234–239. [https://doi.org/10.1016/S0140-6736\(09\)60072-6](https://doi.org/10.1016/S0140-6736(09)60072-6)
- Luck, S. J., & Gold, J. M. (2008). The construct of attention in schizophrenia. *Presented at the Biological Psychiatry*, 64, 34–39. <https://doi.org/10.1016/j.biopsych.2008.02.014>
- Ma, Q., Tang, Y., Wang, F., Liao, X., Jiang, X., Wei, S., Mechelli, A., He, Y., & Xia, M. (2020). Transdiagnostic dysfunctions in brain modules across patients with schizophrenia, bipolar disorder, and major depressive disorder: A connectome-based study. *Schizophrenia Bulletin*, 46(3), 699–712. <https://doi.org/10.1093/schbul/sbz111>
- Maertens, M., & Pollmann, S. (2005). fMRI reveals a common neural substrate of illusory and real contours in V1 after perceptual learning. *Journal of Cognitive Neuroscience*, 17(10), 1553–1564. <https://doi.org/10.1162/089892905774597209>
- Merboldt, K.-D., Finsterbusch, J., & Frahm, J. (2000). Reducing inhomogeneity artifacts in functional MRI of human brain activation—Thin sections vs gradient compensation. *Journal of Magnetic Resonance*, 145(2), 184–191. <https://doi.org/10.1006/jmre.2000.2105>
- Mill, R. D., Gordon, B. A., Balota, D. A., & Cole, M. W. (2020). Predicting dysfunctional age-related task activations from resting-state network alterations. *NeuroImage*, 221, 117167. <https://doi.org/10.1016/j.neuroimage.2020.117167>
- Mur, M., Bandettini, P. A., & Kriegeskorte, N. (2009). Revealing representational content with pattern-information fMRI—an introductory guide. *Social Cognitive and Affective Neuroscience*, 4(1), 101–109. <https://doi.org/10.1093/scan/nsn044>
- Murray, M. M., Imber, M. L., Javitt, D. C., & Foxe, J. J. (2006). Boundary completion is automatic and dissociable from shape discrimination. *Journal of Neuroscience*, 26(46), 12043–12054. <https://doi.org/10.1523/JNEUROSCI.3225-06.2006>
- Noble, S., Mejia, A. F., Zalesky, A., & Scheinost, D. (2022). Improving power in functional magnetic resonance imaging by moving beyond cluster-level inference. *Proceedings of the National Academy of Sciences of the United States of America*, 119(32), e2203020119. <https://doi.org/10.1073/pnas.2203020119>
- O'Donnell, B. F., Swearer, J. M., Smith, L. T., Nestor, P. G., Shenton, M. E., & Mccarley, R. W. (1996). Selective deficits in visual perception and recognition in schizophrenia. *The American Journal of Psychiatry*, 153(5), 687–692. <https://doi.org/10.1176/ajp.153.5.687>
- Peirce, J. W. (2007). PsychoPy—Psychophysics software in python. *Journal of Neuroscience Methods*, 162(1–2), 8–13. <https://doi.org/10.1016/j.jneumeth.2006.11.017>
- Pelli, D. G. (1997). The VideoToolbox software for visual psychophysics: Transforming numbers into movies. *Spatial Vision*, 10(4), 437–442. <https://doi.org/10.1163/156856897X00366>
- Pillow, J., & Rubin, N. (2002). Perceptual completion across the vertical meridian and the role of early visual cortex. *Neuron*, 33(5), 805–813. [https://doi.org/10.1016/S0896-6273\(02\)00605-0](https://doi.org/10.1016/S0896-6273(02)00605-0)
- Pokorny, V. J., Espensen-Sturges, T. D., Burton, P. C., Spohnheim, S. R., & Olman, C. A. (2021). Aberrant cortical connectivity during ambiguous object recognition is associated with schizophrenia. *Biological Psychiatry. Cognitive Neuroscience and Neuroimaging*, 6(12), 1193–1201. <https://doi.org/10.1016/j.bpsc.2020.09.018>
- Power, J. D., Barnes, K. A., Snyder, A. Z., Schlaggar, B. L., & Petersen, S. E. (2012). Spurious but systematic correlations in functional connectivity MRI networks arise from subject motion. *NeuroImage*, 59(3), 2142–2154. <https://doi.org/10.1016/j.neuroimage.2011.10.018>
- Reid, A. T., Headley, D. B., Mill, R. D., Sanchez-Romero, R., Uddin, L. Q., Marinazzo, D., Lurie, D. J., Valdés-Sosa, P. A., Hanson, S. J., Biswal, B. B., Calhoun, V., Poldrack, R. A., & Cole, M. W. (2019). Advancing functional connectivity research from association to causation. *Nature Neuroscience*, 22(11), 1751–1760. <https://doi.org/10.1038/s41593-019-0510-4>
- Rhee, T. G., Olfson, M., Nierenberg, A. A., & Wilkinson, S. T. (2020). 20-year trends in the pharmacologic treatment of bipolar disorder by psychiatrists in outpatient care settings. *The American Journal of Psychiatry*, 177(8), 706–715. <https://doi.org/10.1176/appi.ajp.2020.19091000>
- Ringach, D., & Shapley, R. (1996). Spatial and temporal properties of illusory contours and amodal boundary completion. *Vision Research*, 36(19), 3037–3050. [https://doi.org/10.1016/0042-6989\(96\)00062-4](https://doi.org/10.1016/0042-6989(96)00062-4)
- Rosenberg, M. D., Finn, E. S., Scheinost, D., Papademetris, X., Shen, X., Constable, R. T., & Chun, M. M. (2015). A neuromarker of sustained attention from whole-brain functional connectivity. *Nature Neuroscience*, 19(1), 165–171. <https://doi.org/10.1038/nn.4179>
- Schechter, I., Butler, P. D., Jalbrzikowski, M., Pasternak, R., Saperstein, A. M., & Javitt, D. C. (2006). A new dimension of sensory dysfunction: Stereopsis deficits in schizophrenia. *Biological Psychiatry*, 60(11), 1282–1284. <https://doi.org/10.1016/j.biopsych.2006.03.064>
- Scheinost, D., Noble, S., Horien, C., Greene, A. S., Lake, E. M., Salehi, M., Gao, S., Shen, X., O'Connor, D., Barron, D. S., Yip, S. W., Rosenberg, M. D., & Constable, R. T. (2019). Ten simple rules for predictive modeling of individual differences in neuroimaging. *NeuroImage*, 193, 35–45. <https://doi.org/10.1016/j.neuroimage.2019.02.057>
- Schneider, L. C., & Struening, E. L. (1983). SLOF: A behavioral rating scale for assessing the mentally ill. *Social Work Research & Abstracts*, 19(3), 9–21. <https://doi.org/10.1093/swra/19.3.9>
- Schultz, D. H., Ito, T., Solomyak, L. I., Chen, R. H., Mill, R. D., Anticevic, A., & Cole, M. W. (2018). Global connectivity of the fronto-parietal cognitive control network is related to depression symptoms in the general population. *Network Neuroscience*, 3(1), 107–123. https://doi.org/10.1162/netn_a_00056
- Schulz, M.-A., Yeo, B. T. T., Vogelstein, J. T., Mourao-Miranada, J., Kather, J. N., Kording, K., Richards, B., & Bzdok, D. (2020). Different scaling of linear models and deep learning in UKBiobank brain images versus machine-learning datasets. *Nature Communications*, 11(1), 4238–4215. <https://doi.org/10.1038/s41467-020-18037-z>

- Sehatpour, P., Dias, E. C., Butler, P. D., Revheim, N., Guilfoyle, D. N., Foxe, J. J., & Javitt, D. C. (2010). Impaired visual object processing across an occipital-frontal-hippocampal brain network in schizophrenia: An integrated neuroimaging study. *Archives of General Psychiatry*, 67(8), 772–782. <https://doi.org/10.1001/archgenpsychiatry.2010.85>
- Shen, X., Finn, E. S., Scheinost, D., Rosenberg, M. D., Chun, M. M., Papademetris, X., & Constable, R. T. (2017). Using connectome-based predictive modeling to predict individual behavior from brain connectivity. *Nature Protocols*, 12(3), 506–518. <https://doi.org/10.1038/nprot.2016.178>
- Shipley, W. C., Gruber, C. P., Martin, T. A., & Klein, A. M. (2009). *Shipley-2*. Western Psychological Services.
- Shoham, N., Lewis, G., Hayes, J., McManus, S., Kiani, R., Brugha, T., Bebbington, P., & Cooper, C. (2020). Psychotic symptoms and sensory impairment: Findings from the 2014 adult psychiatric morbidity survey. *Schizophrenia Research*, 215, 357–364. <https://doi.org/10.1016/j.schres.2019.08.028>
- Silverstein, S. M., & Keane, B. P. (2011). Perceptual organization impairment in schizophrenia and associated brain mechanisms: Review of research from 2005 to 2010. *Schizophrenia Bulletin*, 37(4), 690–699. <https://doi.org/10.1093/schbul/sbr052>
- Smith, S. M., Beckmann, C. F., Andersson, J., Auerbach, E. J., Bijsterbosch, J., Douaud, G., Duff, E., Feinberg, D. A., Griffanti, L., Harms, M. P., Kelly, M., Laumann, T., Miller, K. L., Moeller, S., Petersen, S., Power, J., Salimi-Khorshidi, G., Snyder, A. Z., Vu, A. T., ... WU-Minn HCP Consortium. (2013). Resting-state fMRI in the human connectome project. *NeuroImage*, 80, 144–168. <https://doi.org/10.1016/j.neuroimage.2013.05.039>
- Spencer, K. M., & Ghorashi, S. (2014). Oscillatory dynamics of gestalt perception in schizophrenia revisited. *Frontiers in Psychology*, 5(FEB), 68. <https://doi.org/10.3389/fpsyg.2014.00068>
- Spencer, K. M., Nestor, P. G., Perlmuter, R., Niznikiewicz, M. A., Klump, M. C., Frumin, M., Shenton, M. E., & McCarley, R. W. (2004). Neural synchrony indexes disordered perception and cognition in schizophrenia. *Proceedings of the National Academy of Sciences of the United States of America*, 101(49), 17288–17293. <https://doi.org/10.1073/pnas.0406074101>
- Spronk, M., Keane, B. P., Ito, T., Kulkarni, K., Ji, J. L., Anticevic, A., & Cole, M. W. (2020). A whole-brain and cross-diagnostic perspective on functional brain network dysfunction. *Cerebral Cortex*, 31, 547–561. <https://doi.org/10.1093/cercor/bhaa242>
- Sumner, P. (2011). Determinants of saccade latency. In S. Liveridge, I. Gilchrist, & S. Everling (Eds.). *The Oxford handbook of eye movements* (pp. 411–424). Oxford University Press. books.google.com
- Tapia, E., & Breitmeyer, B. G. (2011). Visual consciousness revisited: Magnocellular and parvocellular contributions to conscious and nonconscious vision. *Psychological Science*, 22(7), 934–942. <https://doi.org/10.1177/0956797611413471>
- Teufel, C., Subramaniam, N., Dobler, V., Perez, J., Finnemann, J., Puja, M., et al. (2015). Shift toward prior knowledge confers a perceptual advantage in early psychosis and psychosis-prone healthy individuals. *Proceedings of the National Academy of Sciences*, 1–6, 13401–13406. <https://doi.org/10.1073/pnas.1503916112>
- Valente, G., Castellanos, A. L., Hausfeld, L., De Martino, F., & Formisano, E. (2021). Cross-validation and permutations in MVPA: Validity of permutation strategies and power of cross-validation schemes. *NeuroImage*, 238, 118145. <https://doi.org/10.1016/j.neuroimage.2021.118145>
- van Dellen, E., Börner, C., Schutte, M., van Montfort, S., Abramovic, L., Boks, M. P., Cahn, W., van Haren, N., Mandl, R., Stam, C. J., & Sommer, I. (2020). Functional brain networks in the schizophrenia spectrum and bipolar disorder with psychosis. *NPJ Schizophrenia*, 6(1), 22–29. <https://doi.org/10.1038/s41537-020-00111-6>
- van Mastrigt, S., & Addington, J. (2002). Assessment of premorbid function in first-episode schizophrenia: Modifications to the premorbid adjustment scale. *Journal of Psychiatry & Neuroscience: JPN*, 27(2), 92–101.
- Wallwork, R. S., Fortgang, R., Hashimoto, R., Weinberger, D. R., & Dickinson, D. (2012). Searching for a consensus five-factor model of the positive and negative syndrome scale for schizophrenia. *Schizophrenia Research*, 137(1–3), 246–250. <https://doi.org/10.1016/j.schres.2012.01.031>
- Wokke, M. E., Vandenbroucke, A. R. E., Scholte, H. S., & Lamme, V. A. F. (2013). Confuse your illusion: Feedback to early visual cortex contributes to perceptual completion. *Psychological Science*, 24(1), 63–71. <https://doi.org/10.1177/0956797612449175>
- Wyatte, D., Jilk, D. J., & O'Reilly, R. C. (2014). Early recurrent feedback facilitates visual object recognition under challenging conditions. *Frontiers in Psychology*, 5(4), 760, 674–710. <https://doi.org/10.3389/fpsyg.2014.00674>
- Wynn, J. K., Roach, B. J., Lee, J., Horan, W. P., Ford, J. M., Jimenez, A. M., & Green, M. F. (2015). EEG findings of reduced neural synchronization during visual integration in schizophrenia. *PLoS ONE*, 10(3), e0119849. <https://doi.org/10.1371/journal.pone.0119849.s001>
- Young, R. C., Biggs, J. T., Ziegler, V. E., & Meyer, D. A. (1978). A rating scale for mania: Reliability, validity and sensitivity. *The British Journal of Psychiatry: The Journal of Mental Science*, 133(5), 429–435. <https://doi.org/10.1192/bjp.133.5.429>
- Zhang, Y., & Yang, Y. (2015). Cross-validation for selecting a model selection procedure. *Journal of Econometrics*, 187(1), 95–112. <https://doi.org/10.1016/j.jeconom.2015.02.006>

SUPPORTING INFORMATION

Additional supporting information can be found online in the Supporting Information section at the end of this article.

How to cite this article: Keane, B. P., Krekelberg, B., Mill, R. D., Silverstein, S. M., Thompson, J. L., Serody, M. R., Barch, D. M., & Cole, M. W. (2023). Dorsal attention network activity during perceptual organization is distinct in schizophrenia and predictive of cognitive disorganization. *European Journal of Neuroscience*, 57(3), 458–478. <https://doi.org/10.1111/ejn.15889>